1-1-2003

Reflective in-plane switching liquid crystal displays

Yubao Sun

Zhidong Zhang

Hongmei Ma

Xinyu Zhu
University of Central Florida

Shin-Tson Wu
University of Central Florida

Reflective in-plane switching liquid crystal displays

Cite as: Journal of Applied Physics **93**, 3920 (2003); https://doi.org/10.1063/1.1558967
Submitted: 11 February 2002 . Accepted: 14 January 2003 . Published Online: 21 March 2003

Yubao Sun, Zhidong Zhang, Hongmei Ma, Xinyu Zhu, and Shin-Tson Wu

Reflective in-plane switching liquid crystal displays

Yubao Sun, Zhidong Zhang, and Hongmei Ma
Department of Applied Physics, Hebei University of Technology, Tianjin, 300130, People's Republic of China

Xinyu Zhu and Shin-Tson Wu[a)]
School of Optics/CREOL, University of Central Florida, Orlando, Florida 32816

(Received 11 February 2002; accepted 14 January 2003)

The performance of a reflective in-plane switching (IPS) liquid crystal display is simulated by the parameter space method. The IPS electrodes and reflectors can be separately fabricated on the top and bottom substrates. The normally black reflective in-plane switching display shows wide viewing angle, high contrast ratio, weak color dispersion, and fast response time. © *2003 American Institute of Physics.* [DOI: 10.1063/1.1558967]

I. INTRODUCTION

Liquid crystal displays (LCD) have been used widely in commercial products. Three types of LCD: transmissive, reflective, and transflective, have been developed to meet different application requirements. In the transmissive LCD, a backlight and two polarizers are commonly used. The display exhibits a high contrast ratio ($>300:1$) and good color saturation. In the reflective LCD, the ambient light is used for reading the displayed information. Several reflective LCD have been developed.[1] The mainstream approach uses a single polarizer and a quarter-wave film. Due to the surface and interface reflections, the reflective LCD exhibits a modest contrast ratio ($<50:1$) and color saturation. The major advantage of reflective LCDs is their low power consumption. However, a reflective LCD is difficult to view at dark ambient. To overcome this problem, a transflective LCD has been developed.[2,3] There, a pixel is divided into two subpixels, one responsible for reflective and another for transmissive display. A thin backlight is incorporated into a transflective LCD for using at dark ambient.

Several reflective nematic LCD modes have been investigated. These include twist nematic electrically controlled birefringence mode,[4] hybrid field effect,[5] mixed-mode twist nematic (MTN) cell,[6] and homeotropic (also called vertical-aligned) cell.[7] A general problem of these reflective modes is that their viewing angle is rather narrow ($\sim\pm 40°$). For palm-sized displays, such viewing cone maybe adequate. However, for large screen displays, a much wider viewing cone is required.

The in-plane switching (IPS) mode has been used for large-screen transmissive LCD because of its excellent viewing angle.[8–10] In this article, we extend the IPS mode into reflective liquid crystal displays. We use the parameter space representation method[11] to compute the reflective in-plane switching (R–IPS) mode with a retardation compensation film. In addition to wide viewing angle, the R-IPS mode also exhibits weak color dispersion.

a)Electronic mail: swu@mail.ucf.edu

II. PARAMETER SPACE REPRESENTATION

The parameter space representation is a useful method for optimizing LC cell parameters for a particular LCD.[11] The static optical properties of any reflective nematic LC cell is determined mainly by three parameters: the angle (α) between the polarizer and the front LC director, the liquid crystal twist angle ϕ, and the cell gap-birefringence product $d\Delta n$. Thus, for a given parameter, the reflectance of a LCD can be plotted in a two-dimensional (2D) contour diagram. The Jones matrix for the LC cell with uniform twist and tilt is given by[12–14]

$$M=\begin{pmatrix} A+iB & -C-iD \\ C-iD & A-iB \end{pmatrix}, \tag{1}$$

where

$$A=\cos\phi\cos\beta d+\frac{\phi}{\beta d}\sin\phi\sin\beta d, \tag{2}$$

$$B=\frac{k_\alpha}{\beta}\cos\phi\sin\beta d, \tag{3}$$

$$C=\sin\phi\cos\beta d-\frac{\phi}{\beta d}\cos\phi\sin\beta d, \tag{4}$$

$$D=\frac{k_\alpha}{\beta}\sin\phi\sin\beta d. \tag{5}$$

In Eqs. (2)–(5), ϕ and d are the twist angle and LC cell gap, respectively, and

$$\beta d=[(k_\alpha d)^2+\phi^2]^{1/2}, \tag{6}$$

$$k_\alpha d=\pi\Delta n d/\lambda, \tag{7}$$

here

$$\Delta n=n_e(\theta)-n_o, \tag{8}$$

is the effective birefringence of the tilted liquid crystals, n_o is the ordinary refractive index and $n_e(\theta)$ is the extraordinary index at an average director tilt angle of θ and is given by the following expression:

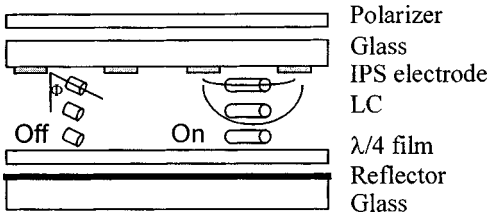

FIG. 1. Device configuration of the proposed reflective IPS display. In the voltage-off state, the LC directors are at an angle Φ with respect to the IPS electrodes.

$$\frac{1}{n_e^2(\theta)}=\frac{\cos^2\theta}{n_e^2}+\frac{\sin^2\theta}{n_o^2}. \tag{9}$$

In the voltage-off state, the tilt angle $\theta\sim 0$. Hence, $\Delta n=n_e-n_o$. At a given wavelength λ, the Jones matrix is completely defined once ϕ and $d\Delta n$ are given.

III. SIMULATION RESULTS

The display configuration we used for simulations is depicted in Fig. 1. It consists of a polarizer, LC cell, a quarter-wave film, and a reflector. It should be mentioned that in the reflective IPS mode, the λ/4 film should be imbedded under the LC layer. If the λ/4 film is sitting between the polarizer and the LC layer, the linearly polarized light (after polarizer) is turned to circularly polarized light after passing the λ/4 film once. As its name implies, in the in-plane switching the LC directors are reoriented in the same plane. Thus, the reflectance is indistinguishable at the voltage off or on states. For an IPS display, the normally black mode is preferred because it provides an excellent dark state at $V=0$. However, the dark state of the normally white mode occurs in a high voltage. Near the IPS electrodes, the LC alignments are disturbed by the electric field resulting in a noticeable light leakage. Thus, the contrast ratio is deteriorated.

In our calculations, we assume that the polarizer makes an angle α and the fast axis of the retardation film makes an angle γ with respect to the front LC director, and δ is the phase retardation value of the compensation film. Under such circumstances, the normalized reflectance (R; by ignoring the optical losses from the polarizer and substrates) of such a display is expressed as follows

$$R=\left|(\cos\alpha,\sin\alpha)\cdot HMH^{-1}FM\cdot\begin{pmatrix}\cos\alpha\\ \sin\alpha\end{pmatrix}\right|^2, \tag{10}$$

here

$$F=\begin{pmatrix}\cos\gamma & \sin\gamma\\ -\sin\gamma & \cos\gamma\end{pmatrix}\begin{pmatrix}e^{-i\delta} & 0\\ 0 & e^{i\delta}\end{pmatrix}\begin{pmatrix}\cos\gamma & -\sin\gamma\\ \sin\gamma & \cos\gamma\end{pmatrix} \tag{11}$$

is the square of the Jones matrix of the retardation film, and

$$H=\begin{pmatrix}\cos\phi & \sin\phi\\ -\sin\phi & \cos\phi\end{pmatrix}. \tag{12}$$

In Eq. (10), HMH^{-1} represents the Jones matrix of the nematic cell with light traveling in the opposite direction. Figure 2(a) shows a contour plot of Eq. (10) with $\alpha=0°$, $\gamma=45°$, and $\lambda=550$ nm, and Fig. 2(b) shows a similar plot with $\alpha=45°$, $\gamma=45°$, and $\lambda=550$ nm. The retardation film is chosen to be a λ/4 film and $\delta=\pi/2$ in Eq. (11). The twist angle ϕ and $d\Delta n$ are used as adjustable parameters.

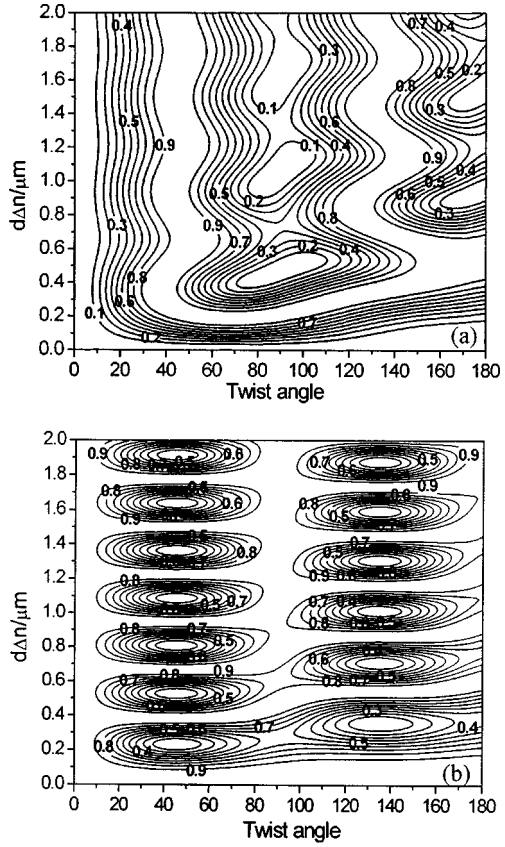

FIG. 2. (a) Solution space for the proposed R–IPS LCD. The polarizer axis and the fast axis of the λ/4 film are at $\alpha=0°$ and $\gamma=45°$, respectively, with respect to the front LC director. The constant reflectivity contours are in step of 10%. (b) Same as (a) except for $\alpha=45°$ and $\gamma=45°$. The constant reflectivity contours are in steps of 10%.

Figure 3 shows the calculated reflectance contours of a homogeneous cell at various polarizer angles and the corresponding $d\Delta n$ values. As shown in Fig. 3, in the voltage-off

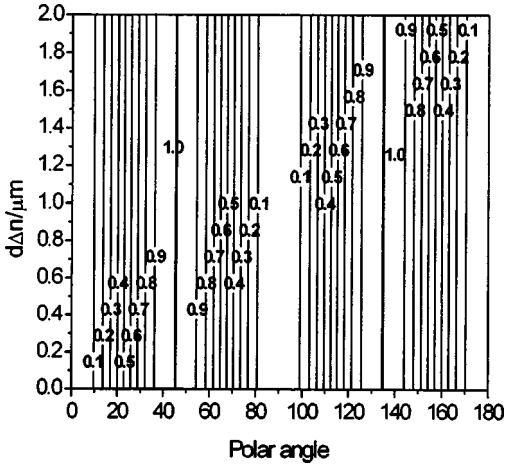

FIG. 3. The calculated reflectance contours of the R–IPS mode using a homogeneous LC cell at various polarizer angles and the corresponding $d\Delta n$ values.

state, the reflectance $R=0$ when $\alpha=0°$ or 90°. This dark state is independent of the $d\Delta n$ value, which implies to a large cell gap tolerance. On the other hand, when $\alpha=45°$ or 135°, $R=1$ regardless of $d\Delta n$.

The earlier analyses correspond to the standard IPS mode employing a homogeneous LC cell, i.e., the twist angle $\phi=0$. The polarizer's axis is parallel to the LC directors. Thus, the incoming linearly polarized light experiences no phase retardation after traversing the LC cell once. After passing the λ/4 film (oriented at 45° to the LC directors) twice, the linearly polarized light remains linear except that its axis is rotated by 90°. At this stage, the returned light polarization is perpendicular to the LC directors. Again, no phase retardation occurs after traversing the LC layer for the second time. The outgoing beam is absorbed by the polarizer resulting in a dark state.

In the voltage-on state, the lateral electric field rotates the LC directors by 45° in order to achieve maximum reflectance. The LC cell and the λ/4 film together function as phase retarders. The total phase retardation Δ, after double pass, should be 2π in order to transmit the polarizer at high efficiency

$$\Delta=2(\delta\pm\pi/2)=2\pi. \tag{13}$$

In Eq. (13), if the on-state LC directors are parallel to the axis of the λ/4 film, then their phase retardations are additive. If orthogonal, then their phase retardations are subtractive. For the interest of minimizing the $d\Delta n$ value, the λ/4 film axis should be oriented parallel to the on-state LC directors so that their phase retardations are additive. Knowing that $\delta=2\pi d\Delta n/\lambda$, we find the lowest order $d\Delta n$ value is λ/4, i.e., the LC layer is a quarter-wave plate. If we optimize the LC cell at $\lambda=550$ nm, then $d\Delta n=137.5$ nm. Under this condition, the 100% reflectance would take place at a very high voltage.

To lower the operating voltage, we could either increase the $d\Delta n$ value, the LC orientation angle (Φ) with respect to the IPS electrodes or increase the dielectric anisotropy of the LC mixture. For a given LC mixture and Φ angle, the on-state voltage is decreased as the cell gap is increased. However, increasing LC cell gap would result in a slower response time. Therefore, the tradeoff between operating voltage and response time should be taken into consideration while designing reflective IPS displays.

Figure 4 plots the voltage dependent reflectance at $\lambda=450$, 550, and 650 nm for the homogeneous LC cell with $d\Delta n=190$ nm, and $\Phi=40°$. These parameters were chosen in order to reduce the on-state voltage to $\sim 5V_{\rm rms}$. The following LC cell parameters are used for simulations: dielectric constants $\varepsilon_{\parallel}=11.4$, $\Delta\varepsilon=7.6$, elastic constants $K_{11}=10$ pN, $K_{22}=7$ pN, $K_{33}=13.6$ pN, birefringence $\Delta n=0.069$ at $\lambda=550$ nm, and rotational viscosity $\gamma_1=0.1$ Pa s, and electrode gap 10 μm. From Fig. 4, the blue wavelength reaches $R=1$ at the lowest voltage, followed by green and red. This is the consequence of the wavelength effect on phase retardation, $\delta=2\pi d\Delta n/\lambda$.

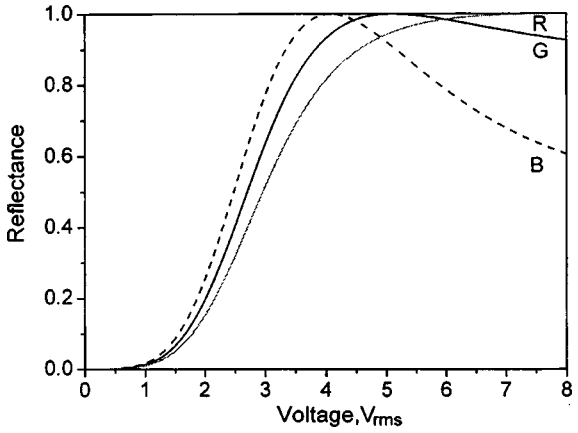

FIG. 4. The voltage-dependent reflectance of the R–IPS cell. $d\Delta n=190$ nm. $\Delta n=0.069$. $\Phi=40°$. Wavelengths $R=650$, $G=550$, and $B=450$ nm.

IV. OBLIQUE ANGLE INCIDENCE

Wide viewing angle is an important requirement for large screen displays. The viewing angle is determined by the contrast ratio at an oblique incident angle θ, and an azimuth angle β. In this article, the azimuth angle $\beta=0$ is defined by the orientation direction of the liquid crystal layer. Only the birefringence of the liquid crystal and the cell gap are changed when the oblique incident angle varies.

An aligned liquid crystal is a uniaxial medium. Its effective birefringence depends on the viewing angle as follows:

$$\Delta n(\theta,\beta)=n_e(\theta,\beta)-n_o, \tag{14}$$

here n_o is the ordinary refractive index and $n_e(\theta,\beta)$ is the extraordinary refractive index. If the incident angle is perpendicular to the optical axis, then $\beta=90°$, and $n_e(\theta,\beta)_{\beta=90°}\equiv n_e$. Under this circumstance, $\Delta n(\theta,\beta)$ is reduced to Δn. If the incident angle is parallel to the optical axis, then $\beta=0°$ and $n_e(\theta,\beta)$ has the following form:

$$n(\theta,\beta)_{\beta=0°}=1/\sqrt{(\sin^2\theta/n_o^2+\cos^2\theta/n_e^2)}, \tag{15}$$

and birefringence is reduced to

$$\Delta n(\theta,\beta)_{\beta=0°}=\frac{n_e n_o}{\sqrt{n_e^2\sin^2\theta+n_o^2\cos^2\theta}}-n_o. \tag{16}$$

For an arbitrary β angle, we can obtain $\Delta n(\theta,\beta)$ by replacing the n_o^2 term in Eq. (16) with $n_e^2(\beta)=1/(\cos^2\beta/n_o^2+\sin^2\beta/n_e^2)$. Besides the birefringence change, the optical path length at angle θ is also increased by a factor of $1/\cos(\theta)$:

$$d(\theta)=d/\cos(\theta). \tag{17}$$

Then the product of d and Δn for any arbitrary angles of θ and β is given as follows:

$$d\Delta n(\theta,\beta)=\frac{d}{\cos\theta}\left(\frac{n_e}{\sqrt{n_e^2\sin^2\theta(\cos^2\beta/n_o^2+\sin^2\beta/n_e^2)+\cos^2\theta}}-n_o\right). \tag{18}$$

V. DISCUSSIONS

In this section, the simulated viewing angle and response time of the reflective IPS mode are presented. Technical challenges on where to implement the IPS electrodes and how to imbed the λ/4 film between the LC layer and reflector are discussed.

A. Viewing angle

Figure 5 plots the isocontrast ratio of the reflective IPS cell with $d\Delta n=190$ nm and $\Phi=40°$. Its viewing angle is quite symmetric. Within the 30° viewing cone, the calculated contrast ratio exceeds 100:1. At $\pm 70°$, the contrast ratio still has 5:1. As compared to the transmissive IPS mode, the R–IPS has a narrower viewing angle. This difference arises from the quarter-wave film employed in the R–IPS. At a large oblique angle, the broadband quarter-wave film is no longer a perfect quarter-wave film. The light leakage occurred at a large oblique angle deteriorates the contrast ratio. On the other hand, in a transmissive IPS LCD, no compensation film is needed. Therefore, the reflective IPS LCD exhibits a narrower viewing angle than the transmissive one.

It should be reminded that during our calculations, all the surface reflections are ignored. The major technical challenge for a reflective display is on the specular reflections. Bumpy reflectors[15] and light control films[16] have been developed for separating the displayed images from specular reflections while steering the reflected ambient light to a designated viewing cone. As a result, the display brightness and contrast ratio are both enhanced.

B. Response time

We also calculated the response time of the 2.75 μm R–IPS cell at eight gray levels. Results are shown in Fig. 6. Owing to the thin cell gap, the rise and decay times are less than 20 ms. In a LCD device, the rise time depends on the applied voltage. The higher the drive voltage, the faster the rise time. Thus, a lower gray level always has a slower rise time. However, the intensity change for a lower gray level is not so significant that our eyes are more forgiven for the slower change.

C. Quarter-wave film

The major technical challenge of the present device configuration is to imbed the λ/4 film between the LC layer and the reflector. In an earlier publication,[17] we have developed a reflective IPS mode with λ/4 sitting between the polarizer and the LC cell. We could laminate the λ/4 film to the polarizer. However, this mode uses an 180°-STN cell and its dark state is relatively sensitive to the cell gap.

The present reflective IPS mode uses a homogeneous cell. Its dark state is insensitive to the cell gap. Ideally, the λ/4 film should be imbedded in the inner side of the bottom substrate in order to avoid parallax. Although challenging, such an approach has been attempted in reflective guest-host[18] and fringing field switching[19] displays. There, the λ/4 film is imbedded beneath the LC cell.

D. IPS electrodes

For the in-plane switching, the electric field is on the transversal direction. In a transmissive IPS LCD, the electrodes are located in the same substrate. However, in a reflective IPS LCD, the reflector has to be imbedded on the inner side of the bottom substrate. In most reflective LCD using longitudinal electric field, the thin-film-transistors are hidden beneath the reflector so that the aperture ratio can exceed 90%.[20] Under such a circumstance, the aluminum

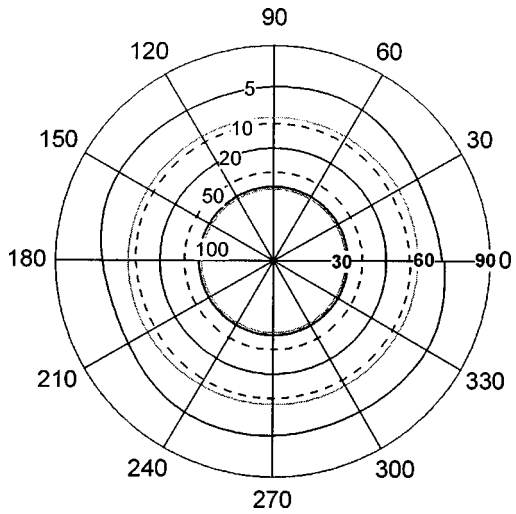

FIG. 5. The calculated isocontrast contours of the R–IPS cell. $d\Delta n=190$ nm.

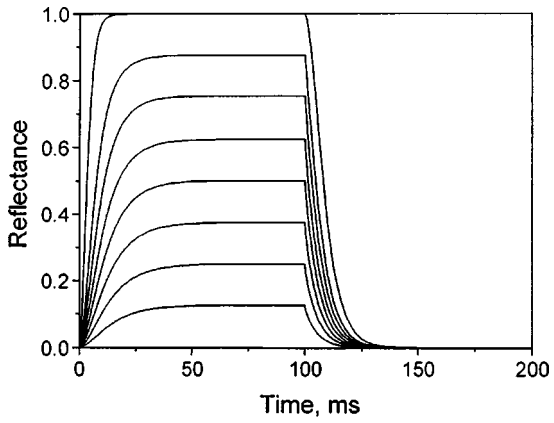

FIG. 6. The calculated response time of the R–IPS cell. Cell gap $d=2.75$ μm. $\Phi=40°$.

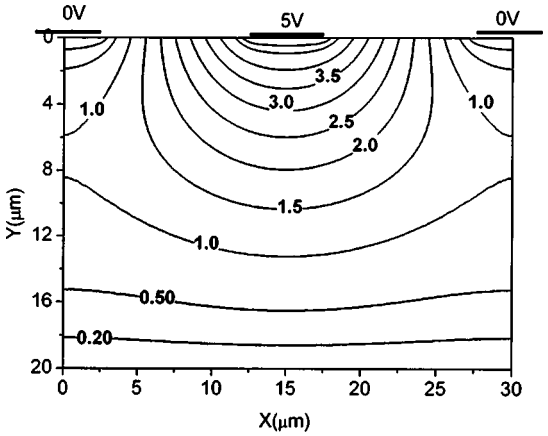

FIG. 7. The voltage distribution between the electrodes and the reflector for the R–IPS cell.

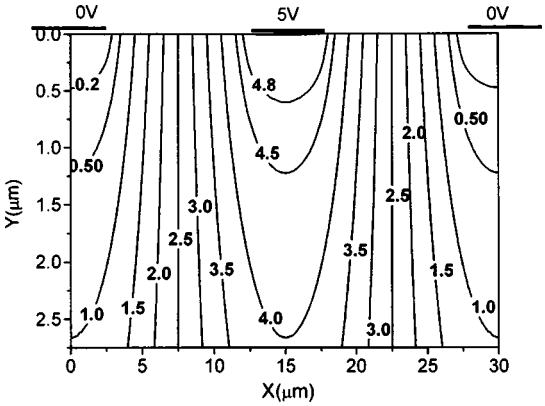

FIG. 9. The voltage distribution for the conventional IPS cell.

reflectors also serve as electrodes. However, in our reflective IPS mode the aluminum reflector and IPS electrodes have to be properly separated.

In Fig. 1, we show a feasible device structure for implementing the reflective IPS mode. The transparent indium tin oxide IPS electrodes are fabricated on the top substrate and the aluminum reflectors are on the bottom substrate. This configuration has been used by the ERSO group for demonstrating a high contrast reflective TFT–LCD using MTN cell.[21,22] The major advantage of this configuration is that the top electrode substrate and bottom reflector substrate can be processed separately. The fabrication process is relatively simple and the manufacturing yield is high. The concern is that whether the metallic reflector distorts the electric field distribution generated by the IPS electrodes. This question is analyzed in detail in the next section.

E. Voltage distribution

In this section, we calculate the voltage distribution with the presence of the aluminum reflector in our mode. As shown in Fig. 1, a λ/4 film is sitting between the LC layer and the reflector. The distance between the IPS electrode and the reflector is the sum of the LC layer and the λ/4 film thicknesses. The effect of the aluminum reflector is determined by the λ/4 film thickness. In our calculations, we assume the λ/4 film has thickness of 17.25 μm and LC layer thickness is 2.75 μm. Thus, the total distance (d) from the electrode to the aluminum reflector is 20 μm.

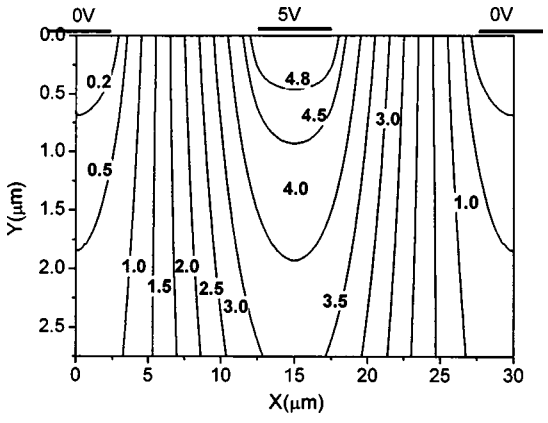

FIG. 8. The voltage distribution in the LC layer for the R–IPS cell.

We calculated the electrical potential using the 2D model. The electrical potential $V(x,y)$ between the electrodes and the reflector is governed by Laplace's equation

$$\nabla^2 V = 0. \tag{19}$$

Using separation of variables and applying the symmetry condition, the periodic condition and the boundary conditions, we obtain the following analytical results:

$$V(x,y) = \frac{V}{2}\frac{d-y}{d} + \frac{4aV}{b}\sum_{n=1}^{\infty}\frac{1}{(n\pi)^2}\cos(n\pi)\sin\left(\frac{n\pi}{2}\right) \times \sin\left(\frac{n\pi b}{2a}\right)\cos\left(\frac{n\pi x}{a}\right)\frac{\sinh\left(\frac{n\pi y}{a}\right)}{\sinh\left(\frac{n\pi d}{a}\right)}. \tag{20}$$

In Eq. (20), a stands for the sum of the electrode width (ω) and the electrode gap (b). Figure 7 shows the voltage distribution with the metallic reflector's distortion in this mode while Fig. 8 shows the voltage distribution only in the LC layer. For comparison, we also calculated the voltage distribution of a conventional IPS cell with the same IPS electrode and cell configuration, except without aluminum reflector. Results are plotted in Fig. 9. Our results are consistent to those reported in Ref. 23. From Figs. 8 and 9, we find that the reflector does not distort the IPS electric field too noticeably.

VI. CONCLUSION

We have analyzed the performances of the proposed reflective IPS configuration. The major advantages of the normally black R–IPS mode are: wide viewing angle, high contrast ratio, large cell gap tolerance, and weak color dispersion. The drawbacks are reduced aperture ratio and lower light efficiency. Imbedding the quarter-wave film between the LC layer and reflector is the major technical challenge.

ACKNOWLEDGMENTS

The authors would like to thank Professor H. S. Kwok of Hong Kong University of Science and Technology for helping the computer drawing programs. The UCF group is indebted to AFOSR for the financial support under Contract No. F49620-01-1-0377.

[1] S. T. Wu and D. K. Yang, *Reflective Liquid Crystal Displays* (Wiley, New York, 2001).
[2] T. Maeda, T. Matsushima, E. Okamoto, H. Wada, O. Okumura, and S. Iino, J. Soc. Inf. Disp. **7**, 9 (1999).
[3] M. Okamoto, H. Hiraki, and S. Mitsui, US Patent No. 6,281,952 B1 (2001).
[4] T. Sonehara and O. Okumura, Proc. Soc. Inf. Display **31**, 145 (1990).
[5] J. Grinberg, A. Jacobson, W. Bleha, L. Miller, I. Fraas, D. Bosewell, and G. Myer, Opt. Eng. **14**, 217 (1975).
[6] S. T. Wu and C. S. Wu, Appl. Phys. Lett. **68**, 1455 (1996).
[7] M. F. Schiekel and K. Fahrenschon, Appl. Phys. Lett. **19**, 391 (1971).
[8] R. A. Soref, J. Appl. Phys. **45**, 5466 (1974).
[9] R. Kiefer, B. Weber, F. Windsceid, and G. Baur, Proceedings of the 12th International Display Research Conference, Hiroshima, Japan, 1992, p. 547.
[10] M. Oh-E and K. Kondo, Appl. Phys. Lett. **67**, 3895 (1995).
[11] H. S. Kwok, J. Appl. Phys. **80**, 3687 (1996).
[12] A. Lien, J. Appl. Phys. **67**, 2853 (1990).
[13] S. T. Tang, F. H. Yu, J. Chen, M. Wong, H. C. Huang, and H. S. Kwok, J. Appl. Phys. **81**, 5924 (1997).
[14] F. H. Yu, S. T. Tang, and H. S. Kwok, J. Appl. Phys. **82**, 5287 (1997).
[15] Y. Itoh, S. Fujiwara, N. Kimura, S. Mizushima, F. Funada, and M. Hijikigawa, SID Tech. Digest **29**, 221 (1998).
[16] Y. P. Huang, F. J. Ko, H. P. Shieh, J. J. Chen, and S. T. Wu, SID Tech. Digest **33**, 870 (2002).
[17] Y. Sun, H. Ma, Z. Zhang and S. T. Wu, J. Appl. Phys. **92**, 1956 (2002).
[18] N. Sugiura and T. Uchida, Soc. Info. Display Tech. Digest **28**, 1011 (1997).
[19] S. H. Lee, S. H. Hong, H. Y. Kim, D. S. Seo, G. D. Lee, and T. H. Yoon, Jpn. J. Appl. Phys., Part 1 **40**, 5334 (2001).
[20] H. Ikeno, H. Kanoh, N. Ikeda, K. Yanai, H. Hayama, and S. Kaneko, SID Tech. Digest **28**, 1015 (1997).
[21] C. L. Kuo *et al.*, SID Tech. Digest **28**, 79 (1997).
[22] C. J. Wen, D. L. Ting, C. Y. Chen, L. S. Chuang, and C. C. Chang, SID Tech. Digest **31**, (2000).
[23] F. Di Pasquale *et al.*, IEEE Trans. Electron Devices **46**, 661 (1999).